Hemagglutinin and neuraminidase containing virus-like particles produced in HEK-293 suspension culture: an effective influenza vaccine candidate

Alina Venereo-Sanchez[a,b], Renald Gilbert[b], Melanie Simoneau[b], Antoine Caron[b], Parminder Chahal[b], Wangxue Chen[c], Sven Ansorge[b], Xuguang Li[d], Olivier Henry[a], Amine Kamen*[e]

[a] *Department of Chemical engineering, Ecole Polytechnique de Montréal, Montréal, Québec, Canada*
[b] *Vaccine Program, Human Health Therapeutics, National Research Council Canada, Montréal, Québec, Canada*
[c] *Human Health Therapeutics, National Research Council Canada, Ottawa, Ontario, Canada*
[d] *Centre for Vaccine Evaluation, Biologics and Genetic Therapies Directorate, HPFB, Health Canada*
[e] *Department of Bioengineering, McGill University, Montréal, Québec, Canada*

**Corresponding author: amine.kamen@mcgill.ca*

A B S T R A C T

Virus-like particles (VLPs) constitute a promising alternative as influenza vaccine. They are non-replicative particles that mimic the morphology of native viruses which make them more immunogenic than classical subunit vaccines. In this study, we propose HEK-293 cells in suspension culture in serum-free medium as an efficient platform to produce large quantities of VLPs. For this purpose, a stable cell line expressing the main influenza viral antigens hemagglutinin (HA) and neuraminidase (NA) (subtype H1N1) under the regulation of a cumate inducible promoter was developed (293HA-NA cells). The production of VLPs was evaluated by transient transfection of plasmids encoding human immunodeficiency virus (HIV) Gag or M1 influenza matrix protein. To facilitate the monitoring of VLPs production, Gag was fused to the green fluorescence protein (GFP). The transient transfection of the gag containing plasmid in 293HA-NA cells increased the release of HA and NA seven times more than its counterpart transfected with the M1 encoding plasmid. Consequently, the production of HA-NA containing VLPs using Gag as scaffold was evaluated in a 3-L controlled stirred tank bioreactor. The VLPs secreted in the culture medium were recovered by ultracentrifugation on a sucrose cushion and ultrafiltered by tangential flow filtration. Transmission electron micrographs of final sample revealed the presence of particles with the average typical size (150-200 nm) and morphology of HIV-1 immature particles. The concentration of the influenza glycoproteins on the Gag-VLPs was estimated by single radial immunodiffusion and hemagglutination assay for HA and by Dot-Blot for HA and NA. More significantly, intranasal immunization of mice with influenza Gag-VLPs induced strong antigen-specific mucosal and systemic antibody responses and provided full protection against a lethal intranasal challenge with the homologous virus strain. These data suggest that, with further optimization and characterization the process could support mass production of safer and better-controlled VLPs-based influenza vaccine candidate.

Keywords: Influenza Vaccine, Virus-Like particles, stable cell line, HEK-293, quantification, bioreactor production, tangential flow filtration.

1. Introduction

Influenza is an illness that causes high morbidity and mortality to human population worldwide [1]. The antigenic “drift” and “shift” phenomena are the origin of the appearance of new strains that cannot be recognized by the host immune system causing severe infections [2, 3]. Thus, every year, seasonal influenza vaccines are produced in embryonated chicken eggs depending on the circulating strains [4].

The production in hen's eggs carries major drawbacks that have been described elsewhere [5, 6]. Additionally, the egg produced seasonal vaccines do not provide full protection in all ages groups [7, 8]. These facts are driving the scientific community to urgently develop a new generation of influenza vaccines that is supported by a robust production platform taking advantages of recent progress in the fields of immunology, molecular and cellular biology, and bioprocessing sciences.

Mammalian cells possess several attractive attributes as a robust production platform candidate due to their ability to perform complex post-translational modifications and the high cell densities reached in suspension cultures in bioreactors. This fact has allowed to increase the platform yields and produce bioproducts of very high quality [6]. Additionally, the required-time to develop stable cell lines has decreased considerably in the past decade. Inducible promotors have been developed in mammalian cells as well, mainly to deal with the overexpression of toxic proteins [9]. The use of inducible promotors also allows to separate the growth phase from the production phase, thereby reducing the metabolic burden during biomass growth [10, 11].

From the perspective of new generation influenza vaccines, different approaches have been investigated to overcome the disadvantages associated to egg produced vaccines [12-19]. Virus-like particle (VLPs) constitute a promising alternative to safely elicit an effective immune response since they mimic native virus [20]. Influenza VLPs have been mostly produced in insect cells. However, this expression platform has the inconvenience of baculovirus contamination in final samples [21]. With the aim of avoiding these drawbacks and exploit the advantages of a superior platform, previous works have explored the production of influenza VLPs in mammalian cells. Most of these studies have been focused in elucidating the virus budding mechanisms [22-25] or testing the protective immunogenicity of VLPs in animals by directly using the sucrose cushion preparations [26, 27]. From a bioprocessing perspective, influenza VLPs have been produced in human embryonic kidney cells (HEK-293) cells but the production levels were significantly lower in comparison with insect cells, and contamination with extracellular vesicles was observed in final samples [28]. In this work, we have developed and characterized an efficient procedure to produce influenza VLPs from a cell clone stably expressing the hemagglutinin (HA) and neuraminidase (NA) of influenza subtype H1N1 (293HA-NA cells). It is demonstrated that HA and NA containing VLPs can be efficiently produced following transfection of the 293HA-NA cells with a plasmid encoding the gag gene of human immunodeficiency virus (HIV) whose product acted as scaffold. The extracellular vesicles were efficiently removed from final preparation by tangential flow filtration (TFF). The Gag-made nanoparticles assembled from 293HA-NA cells showed the typical morphology and expected size for immature HIV-1 particles. An extensive characterization and quantification of the influenza VLPs produced was performed by using different

analytical techniques. The immunogenicity and protective efficacy of the VLPs was demonstrated in mice.

2. Materials and Methods

2.1. Cells, plasmids and antibodies

The cells were cultured in Hyclone SFM4Transfx-293 supplemented with 4-6 mM of glutamine in a humidified incubator at 37 ^{0}C with 5% CO2, at an agitation rate of 100-110 rpm. The gene for M1 (CY033578.1) was codon optimized to human cells and the restriction sites for Hind III were added at both ends of the gene (GenScript) for subsequent cloning in pKCR5 plasmid. The plasmids pUC-HA and pUC-NA H1N1 A/Puerto Rico/8/1934 described in [28] were used as template for PCR to introduce the Kozak sequence and enzymatic sites. A NheI site was introduced toward the 5' end (forward primers 5'-ACTAGCTAGCGCCACCATGAAGGCAAACCTACTGGTCCTG-3'HA and 5'-ACTAGCTAGCGCCACCATGAATCCAAATCAGAAAATAATAACC-3' NA) and HindIII site at the 3' end (reverse primers 5'-ACCCAAGCTTAGATCTTCAGATGCATATTCTGCAC-3' HA and 5'-ACCCAAGCTTAGATCTCTACTTGTCAATGCTGAATG-3' NA). The plasmid pKCR5 contains the CR5 promoter that has been described in [9]. The HIV-1 (HBX2) gag DNA with the Kozak consensus sequence was synthetized by TOPGene Technologies (Canada) and cloned PmeI/NheI in pAdCMV5-GFPq [29] to give rise the plasmid pAdCMV5-gagGFP. The primary antibodies used for the immunofluorescense assay were: Anti-HA LS-C140660 (LifeSpan BioSiences, USA) (I) and Anti-NA ref: 04-230 (NIBSC, UK) (II); for Dot-Blot assay: anti-HA monoclonal produce in-house (III), universal rabbit anti-NA HCA-2 (IV) [30]; for SRID: anti-HA ref: 03/242 (NIBSC, UK) (V); for western blots: (III), (II), Anti-M1 antibody [GA2B] (ab22396) (Abcam, UK) (VI), and anti-GAG monoclonal 2p24 Biotinylated (Hybridoma 31-90-25, ATCC) (VII). The secondary antibodies for the Immunofluorescense assay were #115-495-003 (Jackson Immunoresearch, USA) (VIII) and Alexa Fluor® #594 A11005 (ThermoFisher Scientific, USA) (IX); for Dot-Blot: the infrared-conjugated secondary antibodies IRDye (LI-COR Bioscience, USA); for western blots anti-mouse and anti-sheep IgG-HRP (Jackson Immunoresearch, USA).

2.2. Generation of 293CymR-rcTA cell line

The 293CymR-rcTA cell line was constructed at the National Research Council of Canada (NRC) by stably transfecting the plasmid pMPG-CMV5-CymROpt and pKCMV5-CuO-rcTA in the 293SF-3F6 cell line adapted to serum-free culture [31]. CymR is the repressor and rcTA is the reverse transactivator of the cumate regulation system [9]. The addition of cumate in 293CymR-rcTA cells triggers the synthesis of rcTA and its binding, resulting in the activation of the cumate responsive promoter (CR5).

105 *2.3. Generation of 293HA-NA stable cells*

106 293HA-NA cells were generated by transfecting 1x10^6 cells/ml of 293CymR-rcTA cells with 8µg total
107 DNA of XbaI-linearized plasmids pKCR5-HA, pKCR5-NA and pcDNA6/his-Blasticidin (amount of
108 3:3:2 µg) using PEIpro (Polyplus transfection, France). The selection with Blasticidin S HCl (Enzo Life
109 Sciences, USA) was applied 48 hours post transfection (hpt). Cells were split in 96-well plates with 8-
110 10 µg/ml of Blasticidin. After 3 weeks under selection, several clones were isolated, induced with
111 cumate and screened by Western Blot.
112 The induction of protein expression for all productions in 293HA-NA cells was done at a cell density
113 of 1x10^6 cells/m using 100 µg/ml cumate (stock of 100 mg/ml in Ethanol 70%) (Ark Pharm, Inc., USA).
114 The cultures were stopped at 48-72 h post-transfection.

115 *2.4. Immunofluorescence assay*

116 To perform this assay, 293CymR-rcTA and 293HA-NA cells were seeded at 0.8x10^6 cells/ml in 6-well
117 plates. At 48 h post-induction the culture was centrifuged to discard the supernatant. Cell pellet was
118 washed with 1% ice-cold BSA/PBS (bovine serum albumin/phosphate buffer saline) and incubated in
119 750 µl of this solution for 30 min. Then, 1.5 µL of antibody (I) at 3,7 mg/ml and 2 µL of antibody (II)
120 were added to the cells and incubated for 1h. The cells were washed twice in 1%BSA/PBS. 2.5 µL of
121 VIII and IX secondary antibodies were diluted in 500 µl 1% BSA/PBS and added to the cells for 1h
122 incubation in the dark at 4ºC. Three washes with 1%BSA/PBS were done. The cells were re-suspended
123 in 200 µl 1% ice-cold BSA/PBS and transferred to a glass bottom 4-chamber dish for confocal analysis
124 using a Fluoview FV10i, Olympus microscope.

125 *2.5. 3L-Bioreactor*

126 A 3-L Chemap type SG bioreactor (Mannedorf, Switzerland) was employed to produce the VLPs under
127 controlled and monitored conditions. The bioreactor features have been previously published [5].

128 *2.6. Ultracentrifugation and concentration of VLPs by sucrose cushion 25%*

129 VLPs were concentrated following a protocol that has been previously described elsewhere [28]. All
130 the sucrose cushion samples presented in this work had a concentration factor of 25X.

131 *2.7. Tangential Flow Filtration*

132 The Minimate™ TFF System (PALL Corporation) was used for the ultrafiltration of the influenza Gag-
133 VLPs from the sucrose cushion sample. A Biomax cartridge (1000 kDa 0.005 m^2 PXB01MC50 |
134 Pellicon XL Ultrafiltration Module) was employed in the purification of influenza Gag-VLPs. Before

start the purification the cartridge was sanitized with 0.5 M NaOH overnight. Subsequently, the system was neutralized with SuperQ water. The tubing size used was 16 SI and the retention volume of tubing was measured as 8 ml. Hollow fiber cartridges were used to concentrate control-VLPs and influenza Gag-VLPs recovered from TFF at 1000 KDa cut-off (ref: D02-E300-05-N, D02-E750-05-N, Spectrum Laboratories, USA).

2.8. Cell lysate using RIPA buffer

The cell culture was centrifuged at 1000 rpm for 5 min. The cell pellet was washed twice with 1 ml of PBS1X. The washed pellet was incubated 30 min on ice with 100 µl of RIPA buffer (50 mM Tris-HCl at pH8, 150 mM NaCl 0,1 % SDS, 1% NP-40, 0,25% sodium deoxycholate). Then, the mix was centrifuged at 12000 rpm for 5 min. Samples were analyzed by SDS-PAGE and Western Blot, as previously described [28].

2.9. Dot blot

The protocol followed in this study has been previously published [32]. Briefly, the standards anti-HA and anti-NA employed were hemagglutinin H1N1/A/Puerto Rico/8/34, (Protein Science, USA) and neuraminidase H1N1/A/USSR/90/77, (Sino Biological Inc., China). The detection system used was Odyssey CLx imaging, (LI-COR Bioscience, USA).

2.10. Single Radial Immunodiffusion

The previously published protocol [28] was used and the standard curve was constructed with the same material used for Dot-Blot.

2.11. Hemagglutination assay

The protocol for hemagglutination assay [28] was used. The quantity of VLPs/ml was calculated with the equation:

Viral particle/ml= $[RBC] * 10^{(logHAtiter)}$; where RBC is red blood cells per well ~2x10^6 cells/well

The number of RBCs are proportional to the number of viral particles at the end point dilution. 1 virus=1 RBC [33, 34].

2.12. Determination of host cell proteins and host cell DNA

The HEK-293 host cell proteins (HCP) ELISA kit (Cygnus Technologies, USA) was employed to determine the concentration of HCPs in the samples. The host cell DNA was estimated using the Quant-iT™ PicoGreen® dsDNA Assay Kit (ThermoFisher Scientific, USA).

2.13. Fluorescence intensity measurement and p24 quantification

The supernatant from daily sampling was recovered by centrifugation at 1000 rpm for 5 min. The fluorescence intensity was measured using the Spectrophotometer Synergy H1 BioteK microplate reader set as follows: λ_{em}=485nm and λ_{ex}=528nm. The values graphed were calculated by subtracting the fluorescence intensity values obtained for non-transfected 293CmR-rcTA cells used as negative control. The concentration of p24 was determined using the HIV-1 p24 ELISA assay cat# XB-1000 (XpressBio, USA).

2.14. Transmission electron microscopy (TEM)

Transmission electron micrographs were obtained using a Hitachi H-7500 TEM, operating in high contrast mode at an acceleration voltage of 80kV and at a magnification between 30,000x and 200,000x. Briefly, a 10µL of sample solution was adsorbed to a glow-discharged carbon-coated copper TEM grid (Cu-300HD, Pacific Grid-Tech, CA). Sample was then stained with 10 µL of freshly prepared and filtered 2% uranyl acetate which is applied directly on the grid. After 10 s, the stain was removed by touching the edge of the grid with a filter paper. The grid was dried at room temperature prior to the TEM observation.

2.15. Immunization and viral challenge

Six to eight-week-old female BALB/c mice were purchased from Charles Rivers Laboratories (St. Constant, Quebec). All immunizations were done intranasally at day 0, 14, 21 under lightly anesthesia with isofluorane and using as adjuvant 1 µg cholera toxin (CT, Sigma-Aldrich Canada Ltd., Canada). A group of mice (n=10) was immunized with 50 µl of influenza Gag-VLPs containing 2 µg of HA based on concentration determined by Dot-Blot. Two groups of 5 mice each were immunized with 2 µg of recombinant influenza H1N1 HA (rHA) (A/Puerto Rico/8/34, Sino Biological Inc., USA) or unimmunized (naïve). A group of 7 mice was immunized with control-VLPs containing the same Gag concentration of influenza Gag-VLPs dose. At day 42, five influenza Gag-VLPs immunized mice and 2 control-VLPs immunized mice were sacrificed for blood and nasal lavage fluid collection whereas non-terminal blood samples were collected in 5 rHA-immunized and 5 naïve mice as described elsewhere [35]. All samples were stored at -20ºC until assay. Five weeks after the last immunization, mice were intranasally challenged with 10^3 plaque-forming units (pfu) of the mouse-adapted influenza H1N1 virus (A/Puerto Rico/8/34) in 50 µl PBS. Challenged mice were observed daily for 12 days to monitor body weight and surviving rates.

2.16. Enzyme-linked immunosorbent assay (ELISA) for HA-specific antibodies detection

The 96-wells Immunolon 2R microplates (Thermo Electron Corporation, USA) were coated with 0.2 µg rHA/well in 50 µl of bicarbonate buffer (pH 9.6) at 4ºC overnight. All the subsequent incubations were carried out at room temperature. The plates were blocked with 5% bovine serum in PBS for 1 h, and washed three times with PBS-0.05% Tween 20. Duplicates of 100 µl pre-diluted samples (1:10 for nasal IgA, 1:100 for serum IgA, IgG1 and IgG2a) were added to the wells. After 3 h incubation, alkaline phosphatase-conjugated goat antibodies specific for mouse IgA, IgG1 and IgG2a (Caltag Laboratories, UK) were added and incubated for 1 h. Color reactions were developed by the addition of p-nitrophenyl phosphate (pNPP) substrate (KPL, Inc., USA), and optical density was measured at 405 nm with an automated ELISA plate reader (Synergy H1, Bio-Tek Instruments Inc, USA). Pooled samples collected from mice that had been intranasally immunized with the rHA+CT or from the naïve mice were used as positive or negative controls for the assays, respectively.

3. Results and Discussion

3.1. Development of 293HA-NA stable cells

To generate the 293HA-NA cells the HA, NA and Blasticidin containing plasmids were transfected into the parental cell line 293CymR-rcTA (Fig. 1A). At 48h post-transfection (hpt) cells were maintained under blasticidin selection. Several cell clones were isolated, induced with cumate and the cell lysates were analyzed by Western Blot (data not shown). The clone exhibiting the highest expression levels of HA and NA was selected as our stable 293HA-NA cells. The expression of HA and NA proteins at the surface of the 293HA-NA cells was also confirmed by confocal fluorescence microscopy. The two secondary antibodies employed in the immunoassay were conjugated with two different fluorophore signals: green (NA) and red (HA), respectively (Fig. 1B). The membrane of the cells expressing both proteins turned orange because of the two-color mixed effect. Some cells that are expressing only HA (red membrane) or NA (green membrane) can be observed as well. The non-transfected 293CymR-rcTA cells were treated in the same way and no evidence of non-specific antibody binding was detected (Fig. 1B).

3.2. Comparison of influenza matrix M1 and Gag proteins effect on influenza VLPs production

The effect of two different proteins in triggering the release of VLPs from 293HA-NA cells was studied. There are discrepancies in the literature regarding the role of M1 protein as the driving force for virus budding and assembly [22, 23]. It appears that for influenza virus, the budding process is not driven by a single protein but rather is due to a redundant cooperation among them [2]. For that reason, we

evaluated in parallel the effect of HIV-1 Gag structural polyprotein, which is a well-known protein to promote viral budding of HIV and other viruses including influenza [36-39]. To facilitate the monitoring of Gag expression the protein was fused with the green fluorescent protein.

Thus, three different protein combinations were examined. Co-expression of HA-NA (non-transfected 293HA-NA cells), co-expression of HA-NA-M1 (293HA-NA cells transfected with pKCR5-M1), and co-expression of HA-NA-Gag (293HA-NA cells transfected with pAdCMV5-gagGFP). Since it is expected that VLPs will be released from the cells, a Western Blot analysis was performed to provide first evidence of VLPs presence in the supernatant. The cell lysate was also analyzed. The results showed that co-expression of HA-NA from non-transfected cells released HA in the supernatant while NA expression could not be detected (Fig. 1C). With the combined expression of HA-NA-M1, the detection level of HA in the sucrose cushion was similar to that observed for HA-NA co-expression suggesting no positive impact on protein expression after transfection with M1. The matrix protein M1 was released from the cells, but a larger amount remained trapped within the cells. Our observations support the results obtained by [22] that M1 by itself is not the driving force of influenza virus budding. The presence of M1 in the influenza VLPs seems to influence the functionality and morphology of the VLPs rather than its production [22, 28]. Most likely the current discrepancies in the literature are due to the fact that different expression systems and/or delivery vectors have been employed, which makes it difficult to compare the results [22, 23, 32]. The expression system employed may influence the budding mechanism since the host cell provides the cellular machinery for the viral budding, and many host proteins are found in the VLPs [27].

In contrast with M1, transfection with a gag encoding plasmid was highly efficient to mediate the release of both NA and HA from the cells. This is supported by previous work in insect cells [36]. The expression of HA after HA-NA-Gag co-expression was 7-fold greater than in all previous combinations (HA-NA and HA-NA-M1). This experiment was performed in triplicate and the concentrations of HA and NA after sucrose cushion were estimated by Dot-Blot assay as shown in Table 1.

3.3. Influenza Gag-VLPs production in shake flasks and 3L-Bioreactor

The results obtained in Fig. 1C and Table 1 provided evidences of VLPs production when HA, NA and Gag were co-expressed in the cells. With the goal to assess process scalability, influenza Gag-VLPs production was characterized and compared in shake flasks (50 mL working volume) and fully instrumented bioreactor (3L scale). The timeline for the production process is shown in Fig. 2A. The experiment in shake flasks showed an increase in the fluorescence of supernatant and accumulation of HA protein following transfection/induction (Fig. 2B). The corresponding results obtained in bioreactor are shown in Fig. 2C. While culture performances were overall very similar at both scales, the

fluorescence intensity and HA expression in the supernatant was slightly greater in the bioreactor due to better control of cell culture parameters. The transfection efficiency was found to be 81% in shake flasks and 86 % in bioreactor, as measured by flow cytometry analysis of GFP expressing cells 24 hpt (data not shown). At both scales it was observed a reduction in cell growth rate and viability after transfection/induction, probably due to a toxic effect of PEI [40] and/or Gag protein.

3.4. Tangential Flow Filtration (TFF) of influenza Gag-VLPs

The production of VLPs from mammalian cells is accompanied by extracellular vesicles that contain host cell proteins, DNA and RNA, which are undesired material in a vaccine [28, 41]. Therefore, purification of influenza VLPs is a critical issue to address [42]. In this work, we have evaluated TFF as an important step to remove small extracellular vesicles still present in sucrose cushion sample of Gag-VLPs produced in 293HA-NA cells.

The influenza Gag-VLPs sucrose cushion from the 3L-bioreactor (Feed) was passed through an ultrafiltration cassette with 1000 KDa cut-off. The TFF feed employed was the sucrose cushion since after bioreactor production we aimed testing different purification methods while keeping the aliquots of VLPs well-stored (data not shown). Better process scalability and higher recoveries could be obtained in the future by avoiding centrifugation steps [43]. Thus, the influenza Gag-VLPs sucrose cushion (32 ml) were diafiltered by 4 volume exchanges with a trans-membrane pressure (TMP) kept constant at 8psi. The three proteins HA, NA and Gag were clearly present in the retentate (Fig. 3A). Interestingly, proteins with very low molecular weight were also observed in the TFF retentate suggesting that these small proteins are either part of the influenza Gag-VLPs or adsorbed to the influenza particles (Fig. 3A SDS-PAGE).

The 25% sucrose cushion pellet from supernatant of non-transfected 293CymR-rcTA cells was observed by transmission electron microscopy (TEM) revealing the presence of very small vesicles (10-90 nm) (Fig. 3B). This observation supports the need of more refined process to remove these contaminants from final samples. Fig. 3C and D show the TEM images of influenza Gag-VLPs before and after TFF, respectively. The presence of vesicles clusters and/or cell membrane can be observed in the feed (Fig. 3C). However, after ultrafiltration, the retentate recovered from TFF revealed more pure influenza Gag-VLPs by TEM (Fig. 3D). The size of the influenza Gag-VLPs after TFF ranged from 50-220 nm. TFF using 1000 KDa cut-off membrane appears as a novel approach in the purification of HIV-Gag VLPs, since other studies have reported 300 KDa [44] and 500 KDa [45] cut-off.

3.5. Quantification, characterization and yield of influenza Gag-VLPs

Different methods have been described to quantify HA and NA, the main antigens of influenza virus

[33]. In this study, we have estimated the concentration of HA, NA and Gag proteins in our influenza Gag-VLPs before and after ultrafiltration. The concentration of HA in µg/ml was estimated by Dot-Blot, SRID and its biological activity in HAU/ml was assessed by Hemagglutination assay (Fig. 4). NA and Gag concentrations were determined by Dot-Blot and HIV-1 p24 ELISA, respectively (Fig. 4A). The amount of influenza Gag-VLPs/ml was estimated by correlation with the hemagglutination units. The results obtained from each quantification method are tabulated in Table 1. The slightly differences in concentration obtained by SRID and Dot-Blot could be simply due to intrinsic variability between the techniques or since SRID measures the antigenic conformation of HA [32], there might be less antigenic HA after TFF. The HA units values obtained by the HA assay (8913 HA units/ml) in our final VLPs preparation are greater compared with previous works producing influenza VLPs in mammalian and insect cells [28, 33]. The ratio of NA:HA on the purified Gag-VLPs estimated by Dot-Blot was approximately 1:40, while the ratio obtained for the sucrose cushion preparation of influenza virus H1N1 A/PR/8/34 produced in HEK-293 cells by using the same assay resulted in 1:4 (Table 1). Based on the results of HA concentration by Dot-Blot, the recovery after each step of the influenza Gag-VLPs downstream processing is shown in Table 2. A total HA recovery of 45% was obtained after TFF.

In order to assess the efficiency of the TFF step to remove host cell proteins (HCP) and host cell DNA, the concentration of these contaminants was measured before and after TFF. The results showed that the HCP concentration was 1.3 and 0.49 µg/ml whereas the host cell DNA was 3.7 and 2.46 µg/ml before and after TFF, respectively. These data show that 62.3% of HCP and 33.3% of DNA were removed by TFF.

Finally and with the aim to put our VLPs production process in context with other available recombinant vaccine approaches, the absolute yield and the overall timeline from the moment of receiving the sequence of the new circulating strain until the potential scaled up in a 100L bioreactor and purification has been predicted. Approximately 10 weeks would be required from receiving the DNA sequence until the final selection of the best expressing stable cell clone. Subsequently, 5 weeks might take the cells amplification and VLPs production in a 100L bioreactor. The clarification, TFF and quantification analysis can be performed in one week. Thus, the production of the first bulk of VLPs might take approximately 16 weeks. Certainly, this time could be shortened by further optimizing the production process and by developing a better method to isolate clones [46]. The absolute yield of HA, by SRID, recovered by this process after TFF is 138 µg for 1L of culture volume.

3.6. Immunization and mice challenge protection study

The immunogenicity and protective efficacy of the influenza Gag-VLPs containing HA and NA (H1N1 subtype) were evaluated in mice. Before start the experiment, the VLPs recovered after ultrafiltration by

TFF were 8X concentrated using a hollow fiber cartridge of 300 KDa pore size (purified Gag-VLPs conc.) due to volume restriction for intranasal immunization in animals. The control-VLPs were produced in shake flasks as described in Fig. 2A but by transfecting the pAdCMV5-gagGFP in the parental cell line 293CymR-rcTA instead, such a way there is not HA and NA on the VLPs. The control-VLPs sucrose cushion sample was ultrafiltered and concentrated using 750 KDa and 300 KDa cut-off hollow fiber cartridges, respectively. The concentration of the corresponding proteins in concentrated samples was tabulated in Table 1.

Thus, mice were immunized following the schedule illustrated in Fig. 5A. As shown in Fig. 5B, HA-specific IgA were detected in the nasal lavage fluid of mice intranasally immunized with influenza Gag-VLPs while no or negligible amount of specific IgA was detected in the nasal lavage fluid of mice immunized with the control-VLPs. The fact that our VLPs induced mucosal IgA it is very significant since the respiratory tract is the natural route of influenza virus infection [47]. The serum HA-specific IgA, IgG1 and IgG2a were only detected in mice immunized with influenza Gag-VLPs and the antibody levels were comparable to those in the mice immunized with rHA (Fig. 5B). The detection of IgG1 is an indication of a T helper (Th) type 2 response which has been also observed after vaccination with rHA [48]. Interestingly, the vaccination with influenza Gag-VLPs induced higher titer of IgG2a than the rHA H1N1 vaccinated mice which is associated to a dominant Th1 response [49, 50]. More importantly, the influenza Gag-VLPs immunized mice demonstrated impressive protection against a subsequent lethal intranasal challenge with the homologous virus strain in that the vaccinated mice showed little to no clinical signs or body weight loss throughout the course of infection and all the mice survived the challenge (Fig. 5C). These results suggest that the influenza Gag-VLPs induce a potent protective immunity against lethal influenza virus challenge.

Acknowledgements

The authors would like to thank Viktoria Lytvyn for the precious help with the confocal images and Melanie Leclerc for helping out with the maintenance and freezing of the clones. Authors would like to acknowledge Daniel Jacob for the bioreactor operation and Aziza Manceur for the valuable expert aid with the quantification techniques. We are also grateful of Amalia Ponce for the technical assistance with the immunogenicity and animal study. This work was partially funded through Natural Sciences and Engineering Research Council Grants RGPIN-2015-132; STPGP-462995-14 and Canada Research Chair CRC-240394

References

[1] Rambaut A, Pybus OG, Nelson MI, Viboud C, Taubenberger JK, Holmes EC. The genomic and epidemiological dynamics of human influenza A virus. Nature. 2008;453:615-9.

[2] Rossman JS, Lamb Ra. Influenza virus assembly and budding. Virology. 2011;411:229-36.

[3] Herzog C, Hartmann K, Künzi V, Kürsteiner O, Mischler R, Lazar H, et al. Eleven years of Inflexal V-a virosomal adjuvanted influenza vaccine. Vaccine. 2009;27:4381-7.

[4] Milián E, Kamen AA. Current and emerging cell culture manufacturing technologies for influenza vaccines. BioMed research international. 2015;2015.

[5] Le Ru A, Jacob D, Transfiguracion J, Ansorge S, Henry O, Kamen Aa. Scalable production of influenza virus in HEK-293 cells for efficient vaccine manufacturing. Vaccine. 2010;28:3661-71.

[6] Genzel Y, Behrendt I, Rödig J, Rapp E, Kueppers C, Kochanek S, et al. CAP, a new human suspension cell line for influenza virus production. Applied microbiology and biotechnology. 2013;97:111-22.

[7] Pica N, Palese P. Toward a universal influenza virus vaccine: prospects and challenges. Annual review of medicine. 2013;64:189-202.

[8] Hessel A, Schwendinger M, Fritz D, Coulibaly S, Holzer GW, Sabarth N, et al. A pandemic influenza H1N1 live vaccine based on modified vaccinia Ankara is highly immunogenic and protects mice in active and passive immunizations. PloS one. 2010;5:e12217.

[9] Mullick A, Xu Y, Warren R, Koutroumanis M, Guilbault C, Broussau S, et al. The cumate gene-switch: a system for regulated expression in mammalian cells. BMC biotechnology. 2006;6:43.

[10] Sheikholeslami Z, Jolicoeur M, Henry O. Probing the metabolism of an inducible mammalian expression system using extracellular isotopomer analysis. Journal of biotechnology. 2013;164:469-78.

[11] Aucoin MG, McMurray-Beaulieu V, Poulin F, Boivin EB, Chen J, Ardelean FM, et al. Identifying conditions for inducible protein production in E. coli: combining a fed-batch and multiple induction approach. Microbial cell factories. 2006;5:27.

[12] Lin S-C, Huang M-H, Tsou P-C, Huang L-M, Chong P, Wu S-C. Recombinant trimeric HA protein immunogenicity of H5N1 avian influenza viruses and their combined use with inactivated or adenovirus vaccines. PloS one. 2011;6:e20052.

[13] Smith LR, Wloch MK, Ye M, Reyes LR, Boutsaboualoy S, Dunne CE, et al. Phase 1 clinical trials of the safety and immunogenicity of adjuvanted plasmid DNA vaccines encoding influenza A virus H5 hemagglutinin. Vaccine. 2010;28:2565-72.

[14] Jegerlehner a, Schmitz N, Storni T, Bachmann MF. Influenza A Vaccine Based on the Extracellular Domain of M2: Weak Protection Mediated via Antibody-Dependent NK Cell Activity. The Journal of Immunology. 2004;172:5598-605.

[15] Sedova ES, Shcherbinin DN, Migunov aI, Smirnov Ia, Logunov DI, Shmarov MM, et al. Recombinant influenza vaccines. Acta naturae. 2012;4:17-27.

[16] Kim M-C, Lee Y-N, Ko E-J, Lee JS, Kwon Y-M, Hwang HS, et al. Supplementation of influenza split vaccines with conserved M2 ectodomains overcomes strain specificity and provides long-term cross protection. Molecular therapy : the journal of the American Society of Gene Therapy. 2014;22:1364-74.

[17] Van Kampen KR, Shi Z, Gao P, Zhang J, Foster KW, Chen D-T, et al. Safety and immunogenicity of adenovirus-vectored nasal and epicutaneous influenza vaccines in humans. Vaccine. 2005;23:1029-36.

[18] Alexander J, Bilsel P, del Guercio M-F, Stewart S, Marinkovic-Petrovic A, Southwood S, et al. Universal influenza DNA vaccine encoding conserved CD4+ T cell epitopes protects against lethal viral challenge in HLA-DR transgenic mice. Vaccine. 2010;28:664-72.

[19] Shaw A. New technologies for new influenza vaccines. Vaccine. 2012;30:4927-33.

[20] Chen Q, Lai H. Plant-derived virus-like particles as vaccines. Human vaccines & immunotherapeutics. 2013;9:26-49.

[21] Krammer F, Schinko T, Palmberger D, Tauer C, Messner P, Grabherr R. Trichoplusia ni cells (High Five) are highly efficient for the production of influenza A virus-like particles: a comparison of two insect cell lines as production platforms for influenza vaccines. Molecular biotechnology. 2010;45:226-34.

[22] Chen BJ, Leser GP, Morita E, Lamb RA. Influenza virus hemagglutinin and neuraminidase, but not the matrix protein, are required for assembly and budding of plasmid-derived virus-like particles. Journal of virology. 2007;81:7111-23.
[23] Gómez-puertas P, Albo C, Pe E. Influenza Virus Matrix Protein Is the Major Driving Force in Virus Budding Influenza Virus Matrix Protein Is the Major Driving Force in Virus Budding. 2000;74.
[24] Lai JCC, Chan WWL, Kien F, Nicholls JM, Peiris JSM, Garcia J-M. Formation of virus-like particles from human cell lines exclusively expressing influenza neuraminidase. The Journal of general virology. 2010;91:2322-30.
[25] Wang D, Harmon A, Jin J, Francis DH, Christopher-Hennings J, Nelson E, et al. The lack of an inherent membrane targeting signal is responsible for the failure of the matrix (M1) protein of influenza A virus to bud into virus-like particles. Journal of virology. 2010;84:4673-81.
[26] Tang X-C, Lu H-R, Ross TM. Baculovirus-produced influenza virus-like particles in mammalian cells protect mice from lethal influenza challenge. Viral immunology. 2011;24:311-9.
[27] Wu C-Y, Yeh Y-C, Yang Y-C, Chou C, Liu M-T, Wu H-S, et al. Mammalian expression of virus-like particles for advanced mimicry of authentic influenza virus. PLoS One. 2010;5:e9784.
[28] Thompson CM, Petiot E, Mullick A, Aucoin MG, Henry O, Kamen AA. Critical assessment of influenza VLP production in Sf9 and HEK293 expression systems. BMC biotechnology. 2015;15:31.
[29] Massie B, Mosser DD, Koutroumanis M, Vitté-Mony I, Lamoureux L, Couture F, et al. New adenovirus vectors for protein production and gene transfer. Cell Culture Engineering VI: Springer; 1998. p. 53-64.
[30] Gravel C, Li C, Wang J, Hashem AM, Jaentschke B, Van Domselaar G, et al. Quantitative analyses of all influenza type A viral hemagglutinins and neuraminidases using universal antibodies in simple slot blot assays. Journal of Visualized Experiments. 2011.
[31] Côté J, Garnier A, Massie B, Kamen A. Serum-free production of recombinant proteins and adenoviral vectors by 293SF-3F6 cells. Biotechnology and bioengineering. 1998;59:567-75.
[32] Li C, Jaentschke B, Song Y, Wang J, Cyr TD, Van Domselaar G, et al. A simple slot blot for the detection of virtually all subtypes of the influenza A viral hemagglutinins using universal antibodies targeting the fusion peptide. Nature protocols. 2010;5:14-9.
[33] Thompson CM, Petiot E, Lennaertz A, Henry O, Kamen Aa. Analytical technologies for influenza virus-like particle candidate vaccines: challenges and emerging approaches. Virology journal. 2013;10:141.
[34] Donald HB, Isaacs A. Counts of influenza virus particles. Journal of general microbiology. 1954;10:457-64.
[35] KuoLee R, Harris G, Yan H, Xu HH, Conlan WJ, Patel GB, et al. Intranasal immunization protects against Acinetobacter baumannii-associated pneumonia in mice. Vaccine. 2015;33:260-7.
[36] Haynes JR, Dokken L, Wiley Ja, Cawthon AG, Bigger J, Harmsen AG, et al. Influenza-pseudotyped Gag virus-like particle vaccines provide broad protection against highly pathogenic avian influenza challenge. Vaccine. 2009;27:530-41.
[37] Guo L, Lu X, Kang S-M, Chen C, Compans RW, Yao Q. Enhancement of mucosal immune responses by chimeric influenza HA/SHIV virus-like particles. Virology. 2003;313:502-13.
[38] Haynes JR. Influenza virus-like particle vaccines. Expert review of vaccines. 2009;8:435-45.
[39] Ganser-Pornillos BK, Yeager M, Sundquist WI. The structural biology of HIV assembly. Current opinion in structural biology. 2008;18:203-17.
[40] Ansorge S, Transfiguracion J, Durocher Y, Henry O, Kamen A. Development of a scalable process for high-yield lentiviral vector production by transient transfection of HEK293 suspension cultures. 2009:868-76.
[41] Anastasiadou E, Slack FJ. Malicious exosomes. science. 2014;346:1459-60.
[42] Vicente T, Roldão A, Peixoto C, Carrondo MJT, Alves PM. Large-scale production and purification of VLP-based vaccines. Journal of invertebrate pathology. 2011;107 Suppl:S42-8.
[43] Morenweiser R. Downstream processing of viral vectors and vaccines. Gene therapy. 2005;12 Suppl 1:S103-10.
[44] Cruz PE, Peixoto CC, Devos K, Moreira JL, Saman E, Carrondo MJ. Characterization and downstream processing of HIV-1 core and virus-like-particles produced in serum free medium. Enzyme and microbial technology. 2000;26:61-70.
[45] Negrete A, Pai A, Shiloach J. Use of hollow fiber tangential flow filtration for the recovery and concentration of HIV virus-like particles produced in insect cells. Journal of Virological Methods. 2014;195:240-6.

[46] Caron AW, Nicolas C, Gaillet B, Ba I, Pinard M, Garnier A, et al. Fluorescent labeling in semi-solid medium for selection of mammalian cells secreting high-levels of recombinant proteins. BMC biotechnology. 2009;9:1.
[47] Pyo H-M, Masic A, Woldeab N, Embury-Hyatt C, Lin L, Shin Y-K, et al. Pandemic H1N1 influenza virus-like particles are immunogenic and provide protective immunity to pigs. Vaccine. 2012;30:1297-304.
[48] Bright Ra, Carter DM, Daniluk S, Toapanta FR, Ahmad A, Gavrilov V, et al. Influenza virus-like particles elicit broader immune responses than whole virion inactivated influenza virus or recombinant hemagglutinin. Vaccine. 2007;25:3871-8.
[49] Chen S, Zheng D, Li C, Zhang W, Xu W, Liu X, et al. Protection against multiple subtypes of influenza viruses by virus-like particle vaccines based on a hemagglutinin conserved epitope. BioMed research international. 2015;2015.
[50] Zhang S, Cubas R, Li M, Chen C, Yao Q. Virus-like particle vaccine activates conventional B2 cells and promotes B cell differentiation to IgG2a producing plasma cells. Molecular immunology. 2009;46:1988-2001.

Figure legends

Fig. 1. Development of the 293HA-NA stable cell clone and analysis of VLPs production efficiency. (A) Schematic representation of plasmids pKCR5-HA and NA transfection in the cell line 293CymR-rcTA to create the stable cells 293HA-NA under the cumate regulation system [9]. (B) 72 hours post-induction with cumate, lives cells (no fixation) were observed by confocal microscopy. The arrow points to cell membrane with an orange tone due to simultaneous expression of the two proteins HA and NA. (C) The influence of M1 and Gag proteins on VLPs production from 293HA-NA cells. Lanes (1 and 5) non-transfected 293HA-NA stable cells; (2 and 6) 293HA-NA cells transfected with pKCR5-M1; (3 and 7) 293HA-NA cells transfected with pAdCMV5-GagGFP; (4 and 8) non-transfected parental cell line 293CymR-rcTA as negative control; (C+) sucrose cushion of influenza virus H1N1 A/PR/8/34 produced in HEK-293 cells. The culture supernatants were 25X concentrated through a 25% sucrose cushion and the cells were lysed with RIPA buffer. The same total protein quantity was loaded in each lane, 6 µg for sucrose cushion pellets and 50 µg for cell lysates.

Fig. 2. Gag-VLPs production in shake flasks and 3L-Bioreactor. (A) Diagram of the production process of influenza Gag-VLPs from 293HA-NA cells; (B) and (C) Time course of viable cell growth, cell viability, supernatant HA concentration, and GFP fluorescence intensity in shake flasks and 3L-bioreactor, respectively. The production in shake flask was repeated twice and errors bars shown are standard deviations. The time of transfection was set as 0h. The culture was stopped at 72 hours post-transfection.

Fig. 3. Tangential Flow Filtration (TFF) of influenza Gag-VLPs. (A) SDS-PAGE and Western Blots for HA, NA and Gag detection in the purification steps by TFF. Lanes are (C+) sucrose cushion Influenza virus H1N1 A/PR/8/34 produced in HEK-293 cells; (1) The feed which is sucrose cushion from supernatant of 3L-bioreactor influenza Gag-VLPs production; (2) Permeate; (3) Retentate which is referred as "purified influenza Gag-VLPs". The reducing agent used was DTT at 168 mM and samples were boiled for 5 min at 95ºC. The position of the relevant proteins is marked with an arrow according to their expected molecular weight and the detection by Western Blot (B) Transmission electron microscopy (TEM) image 20,000 X of 25% sucrose cushion from parental cell line 293CymR-rcTA supernatant. TEM images 20,000X (C) Feed and (D) Purified influenza Gag-VLPs. Black arrows highlight the influenza Gag-VLPs, white arrows point to vesicles and striped arrow indicates vesicles clusters. The VLPs are identified as the particles showing the classical dense core structure and morphology of HIV, whereas the vesicles are those lacking of the dense core with more irregular shapes. A total of 10 different field images at different magnifications were taken of the purified influenza Gag-VLPs and none of them showed presence or traces of vesicles or vesicles cluster.

Fig. 4. Quantification of HA and NA on influenza Gag-VLPs before and after TFF. (A) Dot-Blot using anti-HA and anti-NA antibodies. (Standard) Hemagglutinin recombinant protein from H1N1 A/Puerto Rico/8/34 (10 µg/ml top dot) and neuraminidase recombinant protein from H1N1 A/USSR/90/77 (2.5 µg/ml top dot); (Feed) sucrose cushion from supernatant of 3L-bioreactor influenza Gag-VLPs production used as feed in the TFF, dilutions from ½ to 1/256 (top to bottom); (Purified

Gag-VLPs) Retentate from TFF; (Ctrl -) sucrose cushion from 293CymR-rcTA cells supernatant, dilutions from ½ to 1/256 (vertical from top to bottom). (B) Single radial immunodiffusion (SRID) (Standard) same than for Dot-Blot anti-HA, horizontal dilutions from 30-7.5 µg/ml; samples horizontal dilutions from (2/3 to 1/8). The arrows are pointing to the periphery of the rings (C) Hemagglutination assay. Samples were diluted 1/10 in PBS, then sequentially diluted by 10.

Fig. 5. Immunity of influenza Gag-VLPs and mice challenge. (A) Vaccination schedule. (B) Sera IgG and/or nasal IgA specific to VLPs were evaluated by ELISA. At day 42, the nasal fluid and blood from sacrificed mice of groups immunized with (2µg HA) influenza Gag-VLPs and control-VLPs were analyzed for nasal IgA and sera IgA, IgG1, and IgG2a response. Non-terminal blood samples from 2 µg rHA H1N1-immunized and naïve mice were assayed for HA-specific IgG sera antibodies. Each individual dot represents the value from a single mouse, and the horizontal line represents the median value for the group. The concentration of HA used per dose was based on the Dot-Blot assay results (C) Five weeks after last immunization, mice of all groups were intranasally challenged with 10^3 pfu of the mouse-adapted influenza H1N1 virus (A/Puerto Rico/8/34). The percentages of body weight (BW) changes and survival were daily recorded for up to 12 days. Body weight data are the means for five mice per group ± SD.

Table 1. Summary of HA, NA and Gag quantification

Samples	Dot-Blot (µg/ml)		SRID (µg/ml)	HA assay (HAU/ml)	ELISA (ng/ml)	Based on HA assay
	HA	NA	HA	HA	p24	VLPs/ml
HA-NA	1.18 ± 0.14	0.05 ± 0.01	-	-	N/A	-
HA-NA-M1	1.19 ± 0.38	0.08 ± 0.00	-	-	N/A	-
HA-NA-Gag	7.59 ± 0.21	0.40 ± 0.02	-	-	-	-
TFF Feed	8.41	0.4	9.2	12589	28.8	$2.52x10^{10}$
Purified Gag-VLPs	6.05	0.16	3.4	8913	25.7	$1.78x10^{10}$
Purified Gag-VLPs conc.	42	1.86	30.2	-	178.4	-
Control-VLPs	N/A	N/A	N/A	N/A	100.8	N/A
H1N1 A/Puerto Rico/8/34	80	19.62	-	-	-	-

**(N/A) non-applicable*
**(-) not measured*

Table 2. Recovery of the purification by TFF based on anti-HA Dot-Blot results

Samples	Volume (ml)	HA (µg/ml)	Total HA (µg)	Recovery (%)
Supernatant 3L-bioreactor (before clarification)	800	0.54	432	100
TFF Feed	32	8.41	269.12	62.3
Purified Gag-VLPs	32.4	6.05	196.02	45.4

529 **Figure 1**

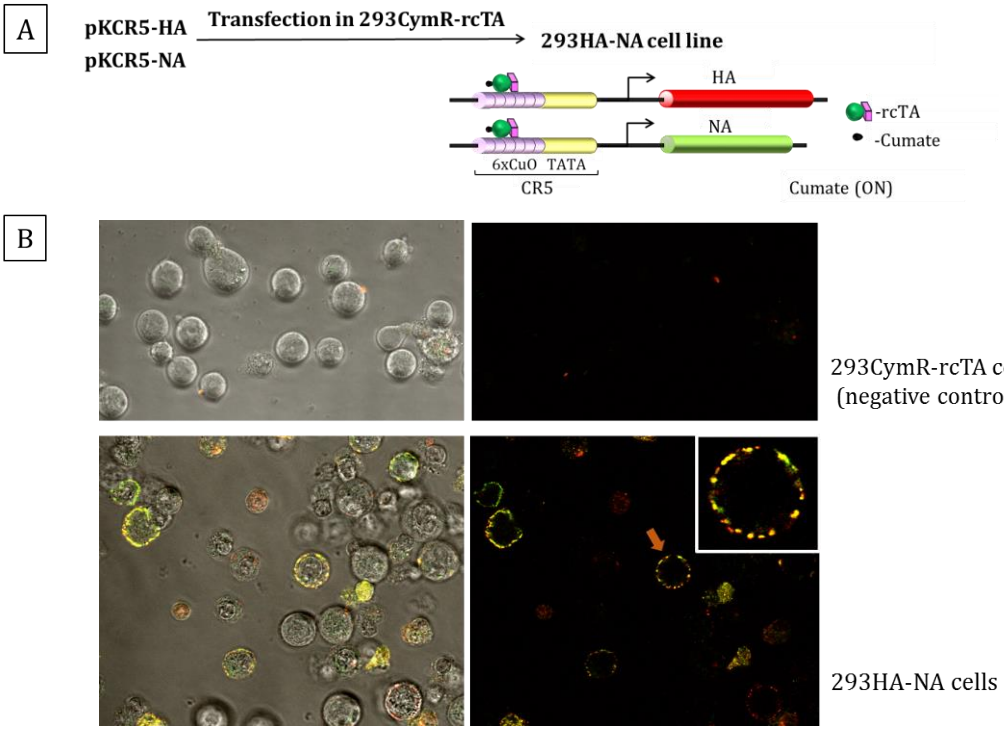

530

531 **Figure 2**

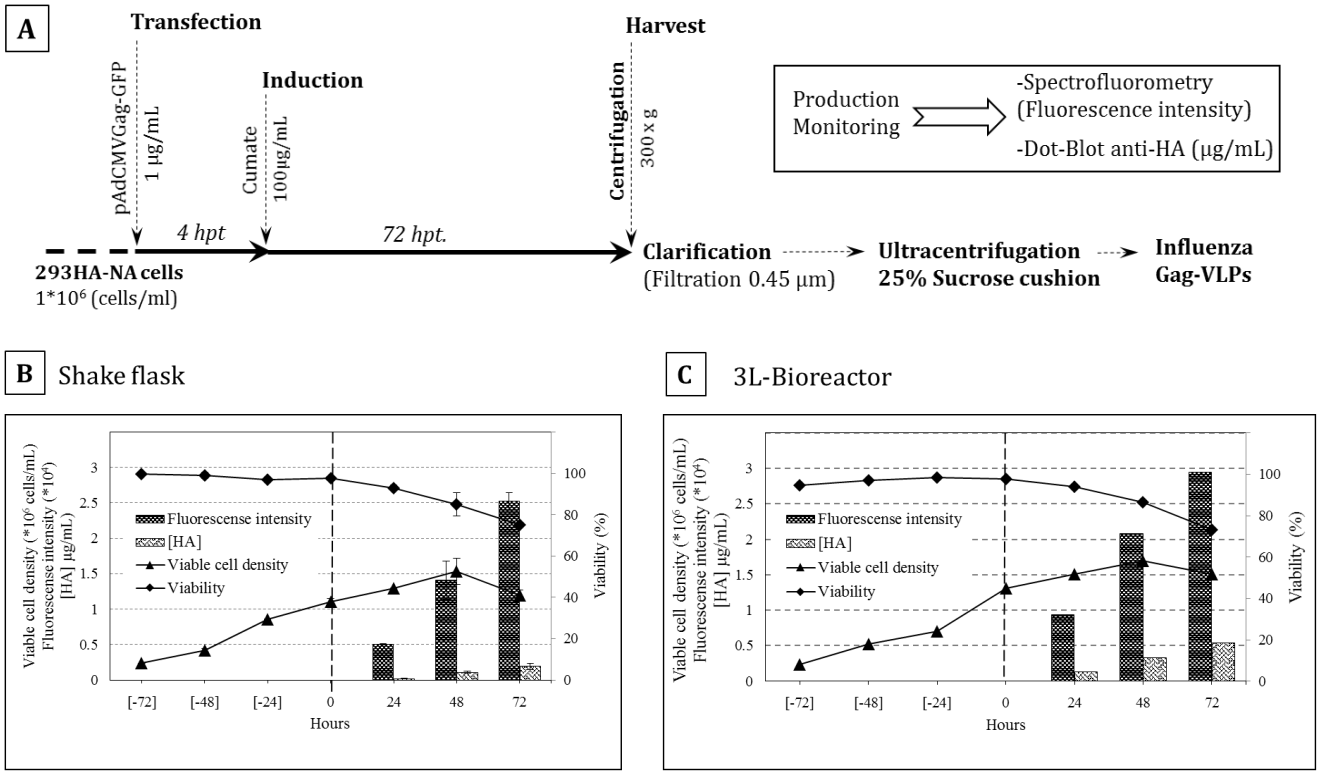

532

533

534 **Figure 3**

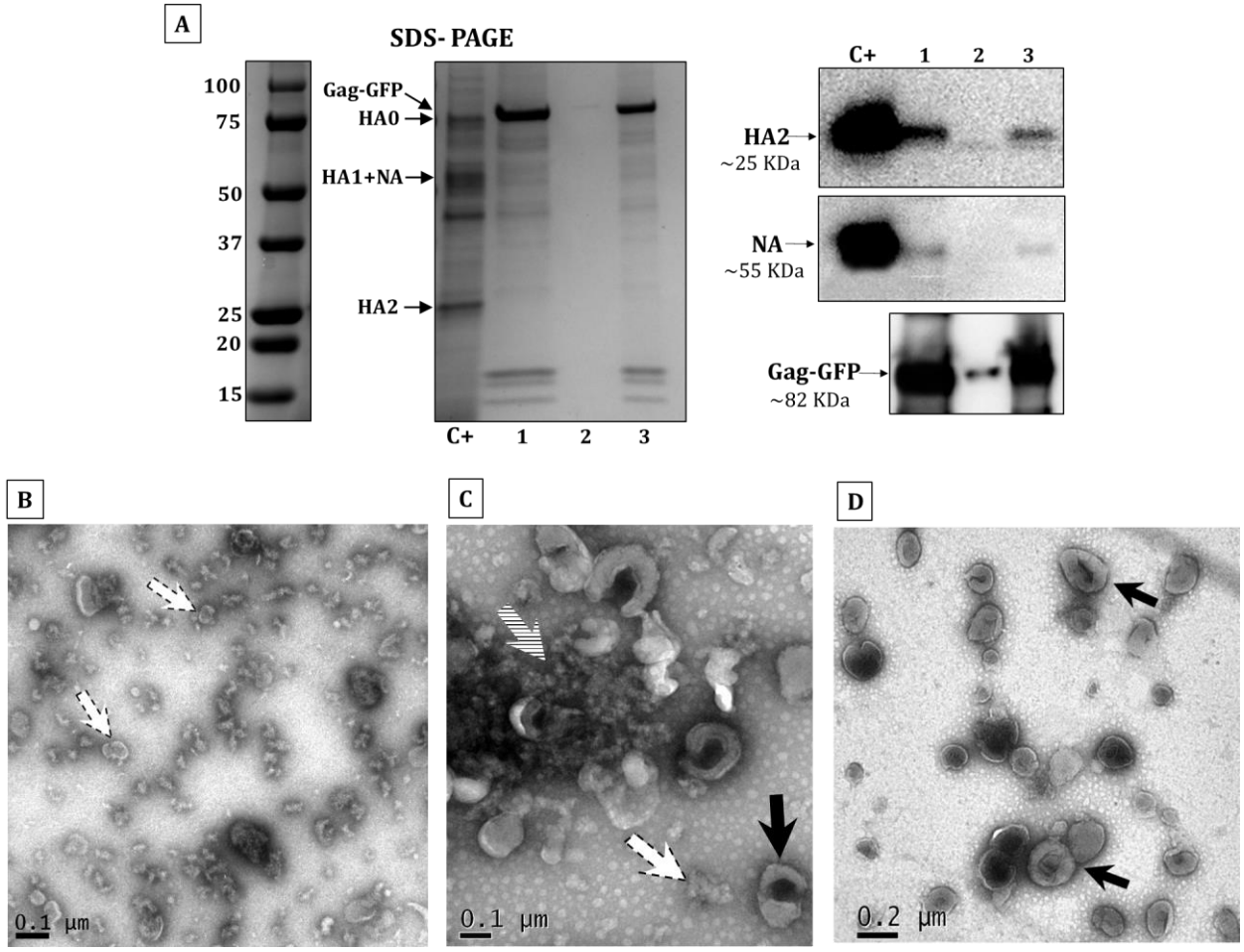

535

536

537 **Figure 4**

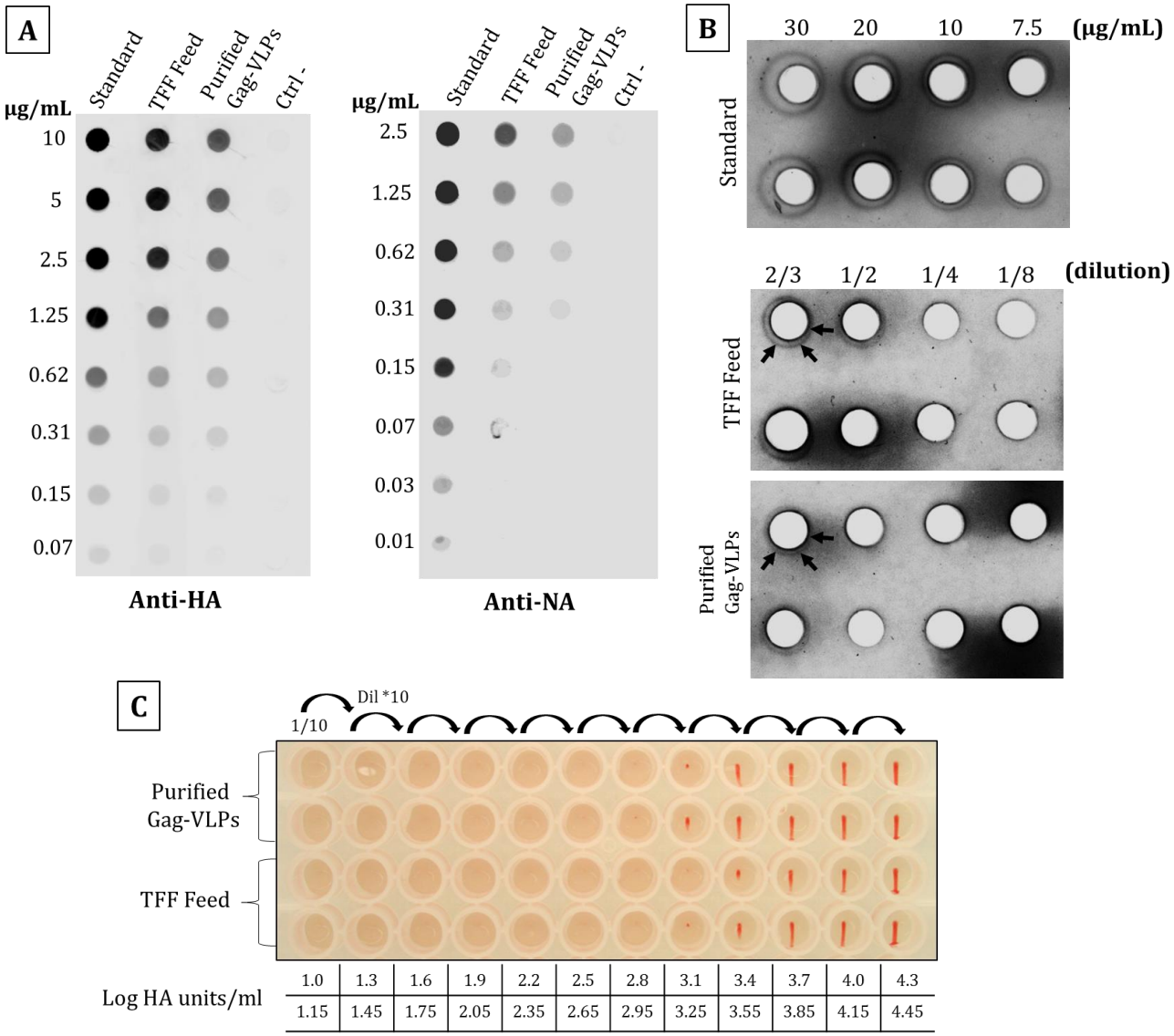

538

539

540

541 **Figure 5**

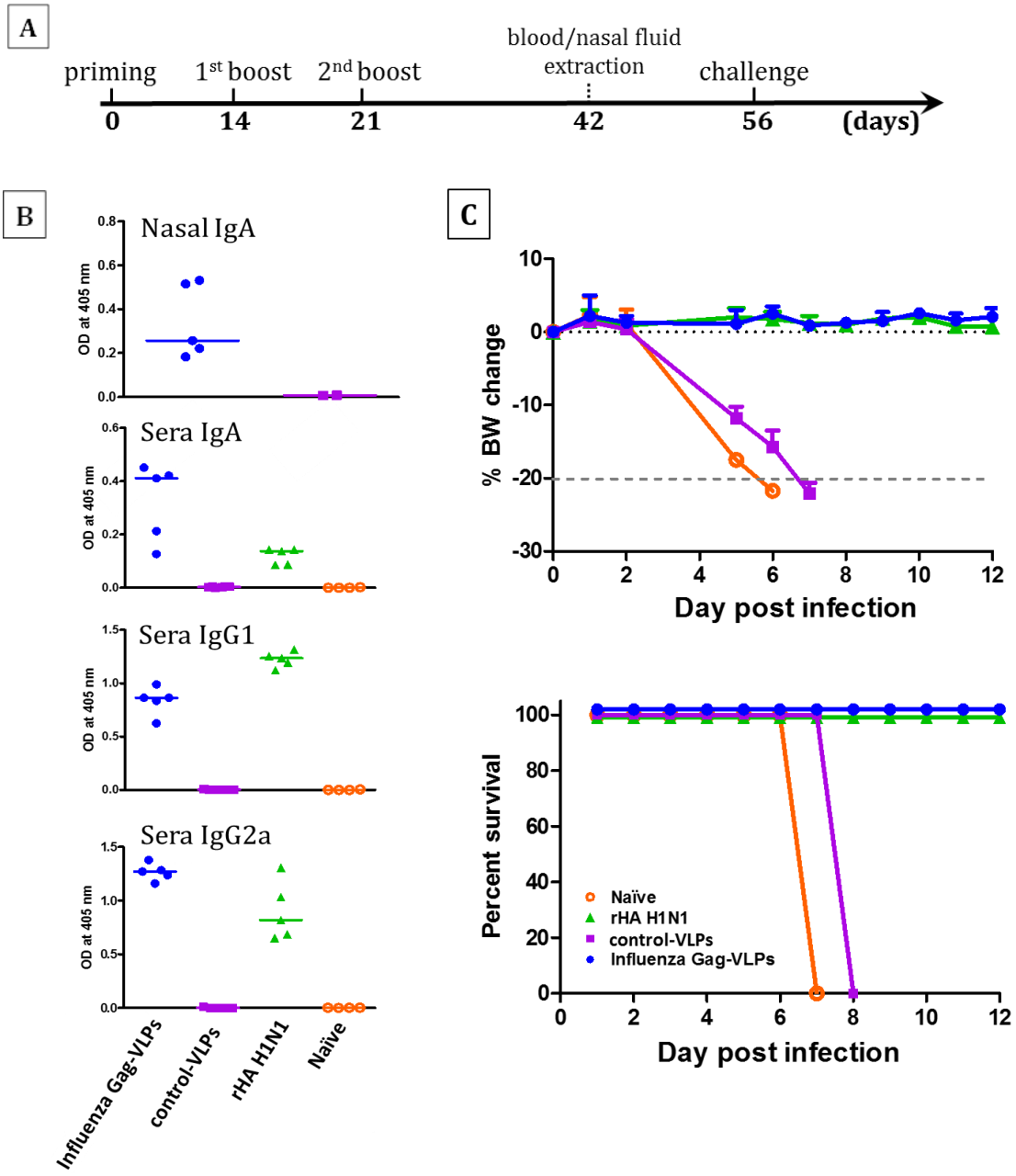

542

543